Supporting information for

Mesostructured amorphous manganese oxides: facile synthesis and highly durable elimination of low-concentration NO at room temperature in air

Yanyan Du, Zile Hua*, Weimin Huang, Meiying Wu, Min Wang, Jin Wang, Xiangzhi Cui, Lingxia Zhang, Hangrong Chen and Jianlin Shi*
State Key Lab of High Performance Ceramics and Superfine Microstructure, Shanghai Institute of Ceramics, Chinese Academy of Sciences, 1295 Dingxi Road, Shanghai 200050, P R China.
E-mail: jlshi@mail.sic.ac.cn (J.Shi); huazl@mail.sic.ac.cn (Z.Hua);

Materials

Potassium permanganate ($KMnO_4$, A.R.) and oxalic acid dihydrate ($C_2H_2O_4 \cdot 2H_2O$, A.R.) were purchased from Sinopharm Chemical Reagent Co. Ltd. All the materials are used without further purification.

Synthesis procedures

AMO was prepared by the reaction of potassium permanganate and oxalic acid at room temperature. In a typical run, 1.58 g $KMnO_4$ was dissolved in 60 mL deionized water and 1.89 g $H_2C_2O_4 \cdot 2H_2O$ was dissolved in 100 mL deionized water, respectively. Then the potassium permanganate solution was added dropwise into the oxalic acid solution under stirring. The resulting mixture was kept stirring for 8 ~ 48 h at room temperature. Then the brown slurry was filtered and washed with deionized water for three times and dried at 120 ^oC overnight. The obtained materials were denoted as Mn-*t*h, in which ***t*** represents the reaction time duration.

Honeycomb ceramics with the constituent of $2MgO\text{-}2Al_2O_3\text{-}5SiO_2$ were purchased from Shanghai Pengyi Material Co. Ltd. The monolithic honeycomb was cylindrical (50 mm in diameter and 50 mm in length), and the cell density was 400 cells per square inch. The monolith pieces are coated by Al_2O_3 and then annealed at 550 ^oC overnight.

NO removal test

The NO removal tests were carried out in a quartz tubular fixed-bed flow reactor with an inner diameter of 8 mm, which was maintained at 25 °C by a thermostatic water bath. The reactant gas composition was 10 ppm NO, 21% O_2 and balance N_2 or 10 ppm NO with fresh air (relative humidity 50~90%, in simulation to the typical air conditions in road tunnels and underground parks) as carrier gas. In each test, 0.1 g catalyst was used and the total flow rate was controlled at 200 $mL \cdot min^{-1}$, corresponding to a space velocity of 120,000 $mL \cdot g^{-1} \cdot h^{-1}$. The NO and NO_x (NO_x = NO + NO_2) concentrations in the inlet and outlet gas were online monitored by the NO_x analyzer (Thermo Fisher 42i-LS). The NO removal ratio was calculated using equation (1), where NO_{inlet} and NO_{outlet} are the NO concentrations in the inlet and outlet gas, respectively.

$$\text{NO removal test}\,(\%) = \frac{NO_{inlet} - NO_{outlet}}{NO_{inlet}} \times 100 \qquad (1)$$

Catalysts characterization

X-ray diffraction (XRD) patterns were recorded on a Rigaku D/Max 2200 PC diffractometer using Cu Kα radiation at 40 kV and 40 mA at room temperature by step scanning in the angle range of $5° \le 2\theta \le 80°$ with increments of 0.02°. Nitrogen adsorption and desorption isotherms at

77 K were measured on a Micromeritics TriStar 3020 porosimeter. All samples were pretreated at 150 °C for 6 h under flowing nitrogen before measurements. The specific surfaces areas were calculated with the Brunauer-Emmet-Teller (BET) methods. Fourier transform infrared (FTIR) spectra were recorded with a Nicolet iS10 FTIR spectrometer. X-ray photoemission (XPS) measurements were carried out using a Thermo Fisher Scientific ESCALAB 250.

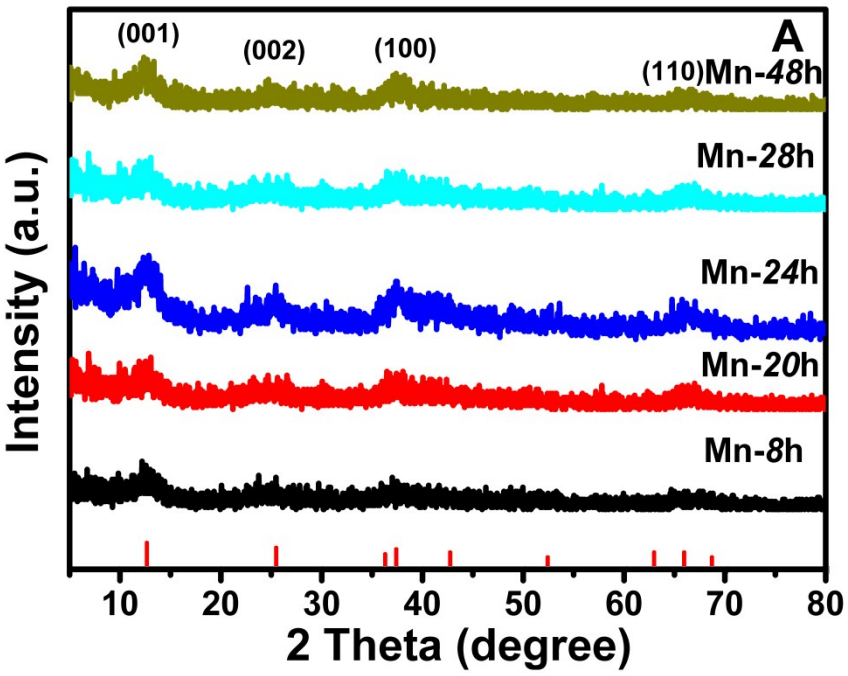

Figure S1. XRD patterns of catalysts synthesized under different conditions. Red vertical lines indicate the standard XRD patterns of K^+-birnessite.

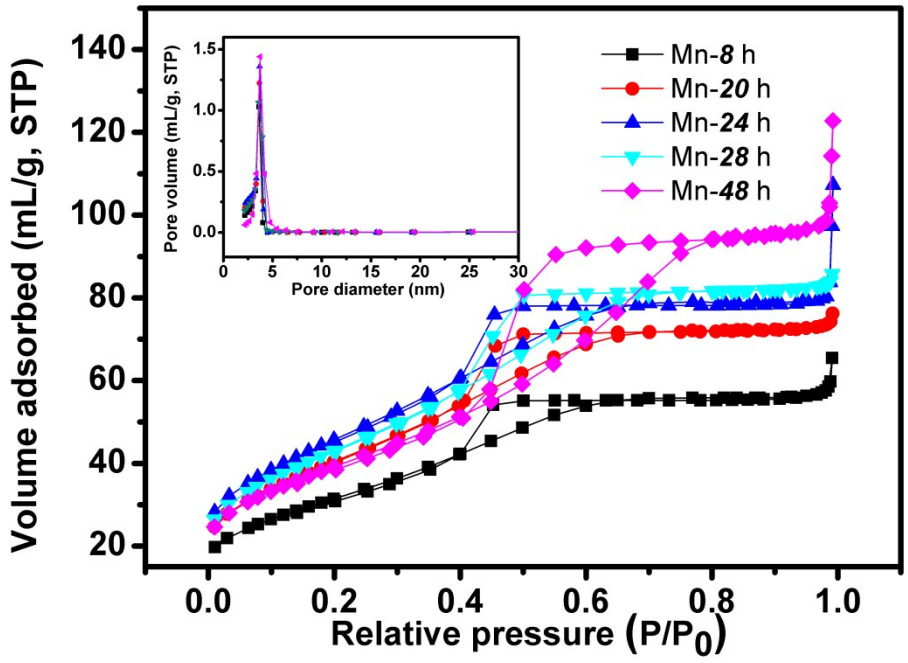

Figure S2 N_2 adsorption-desorption isotherms and BJH desorption pore size distribution plots (inset) of Mn-***t***h.

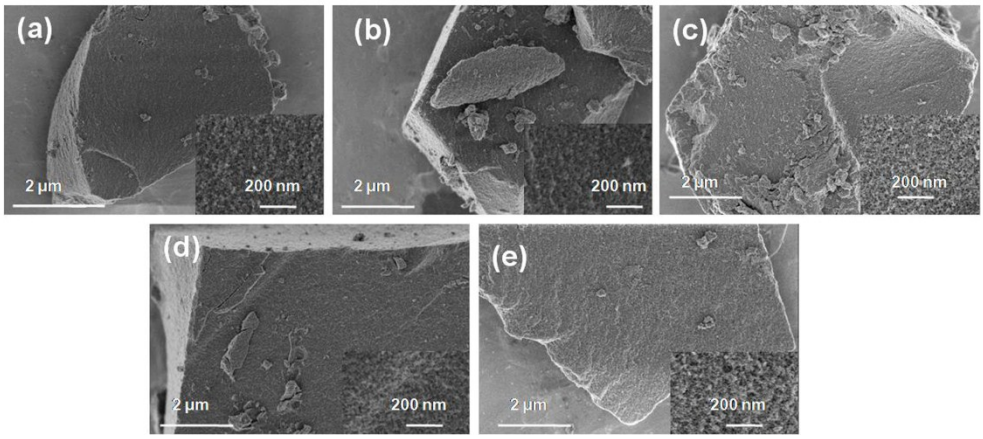

Figure S3 SEM images of (a) Mn-***8***h, (b) Mn-***20***h, (c) Mn-***24***h, (d) Mn-2***8***h and (e) Mn-***48***h.

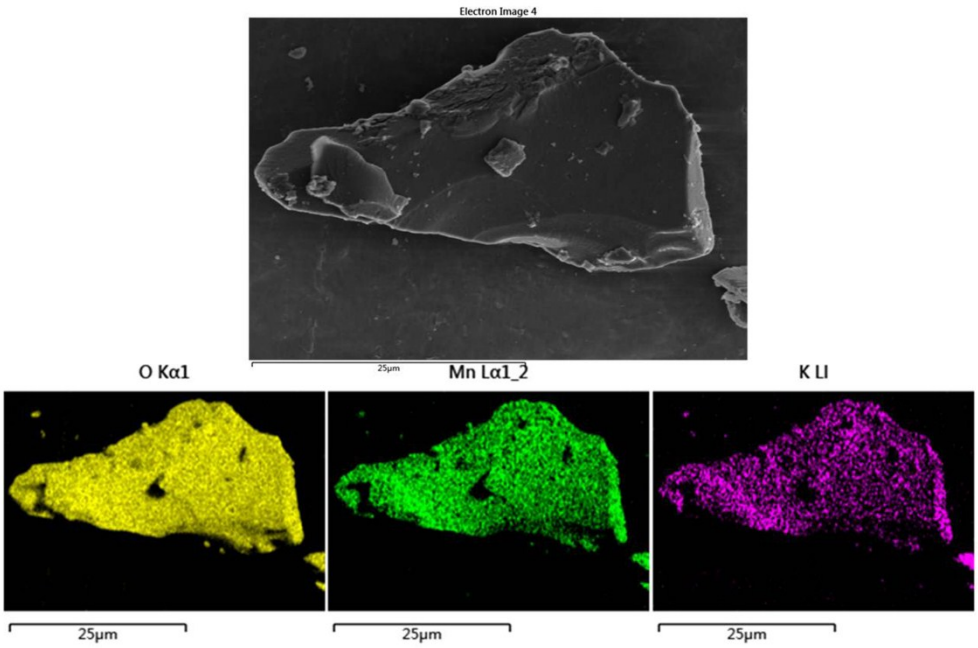

Figure S4 Element mapping of O, Mn and K in Mn-***24***h.

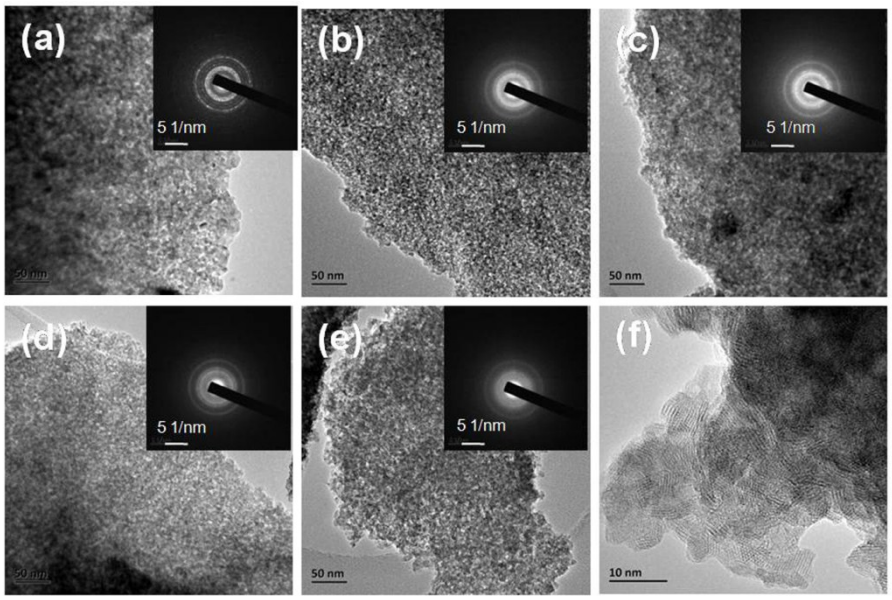

Figure S5 TEM images and diffraction patterns of (a) Mn-***8***h, (b) Mn-***20***h, (c) Mn-***24***h, (d) Mn-***28***h and (e) Mn-***48***h. (f) HRTEM image of Mn-***24***h.

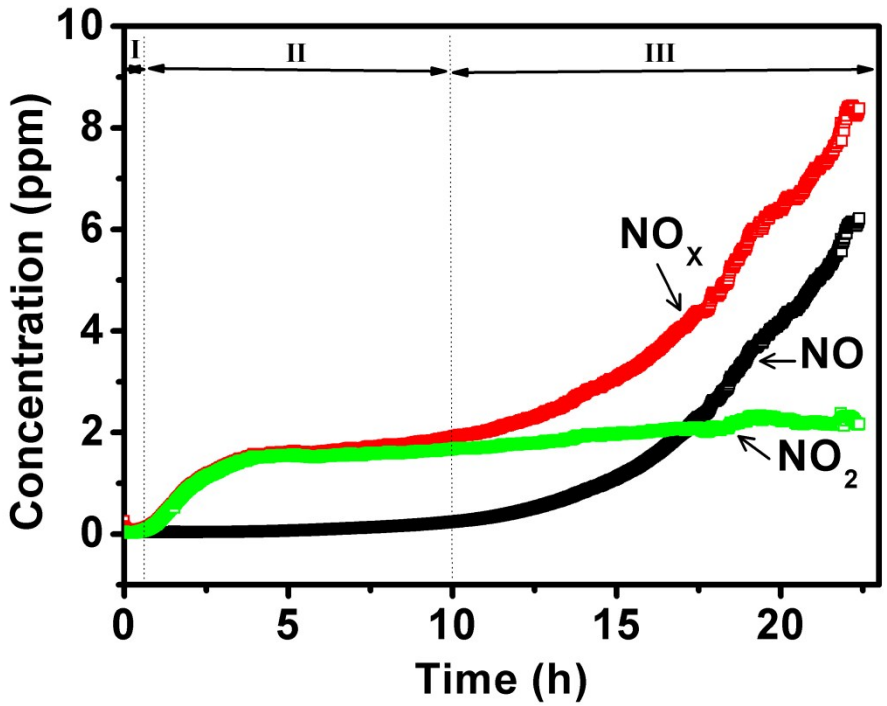

Figure S6 Time courses of outlet NO, NO_2 and NO_x concentrations of the sample Mn-***24***h during the NO removal test. Reaction conditions: [NO] = 10 ppm, [O_2] = 21%, balance = N_2, temperature = 25 ℃ and space velocity = 120,000 mL·h^{-1}·g^{-1}.

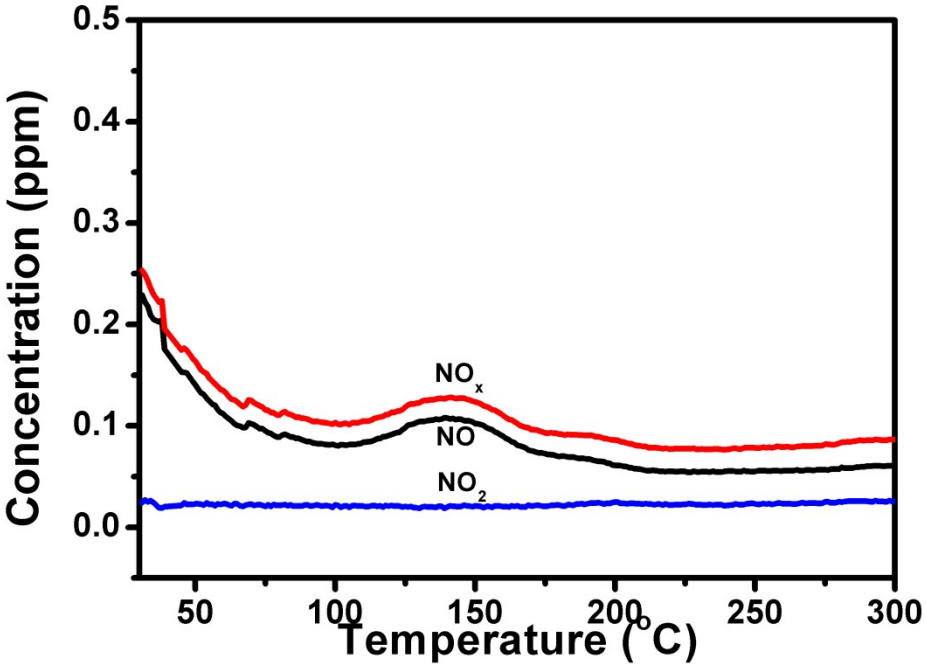

Figure S7 TPD curves of Mn-*24*h after 237 h of NO removal tests under humid condition.

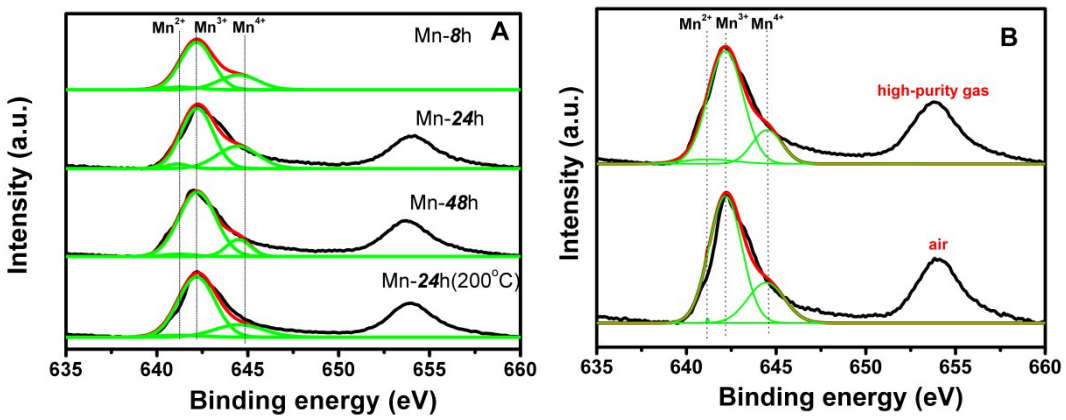

Figure S8 XPS spectra of Mn 2p of synthesized Mn-***t***h samples (A) and used Mn-***24***h after the NO removal test with high-purity gas and fresh air as the carrier gas, respectively.

In Figure S8, the two peaks with the binding energy at 642.2 eV and 653.9 eV corresponded to Mn $2p_{3/2}$ and Mn $2p_{1/2}$, respectively. Peak fitting was carried out for Mn $2p_{3/2}$, deconvoluted into Mn^{2+}, Mn^{3+} and Mn^{4+} with the characteristic binding energy at 641.2 eV, 642.2 eV and 644.5 eV, respectively. The corresponding distributions of Mn^{2+}, Mn^{3+} and Mn^{4+} are listed in Table S3. It is clear that the amount of Mn^{2+} is very low and the percentages of Mn^{4+} are 26.2%, 30.2% and 14.7% for Mn-***8***h, Mn-***24***h and Mn-***48***h, respectively. More significantly, when the best performed catalyst Mn-***24***h was annealed at 200 °C for 6 h (Mn-***24***h(200 °C)), its percentage of Mn^{4+} decreased from 30.2% to 20.7% and consequently it became completely inactive and inferior to that of Mn-***8***h, as shown in Figure S8A and Table S3. After the NO removal tests using high purity carrier gases or fresh air carrier gas (relative humidity of 50~90%), the XPS spectra were recorded and shown in Figure S8B. For

the used Mn-*24*h samples using fresh air as the carrier gas, the percentage of Mn^{4+} was almost unchanged while it greatly decreased for the one using high purity carrier gases, which is in accordance with the NO removal performance results.

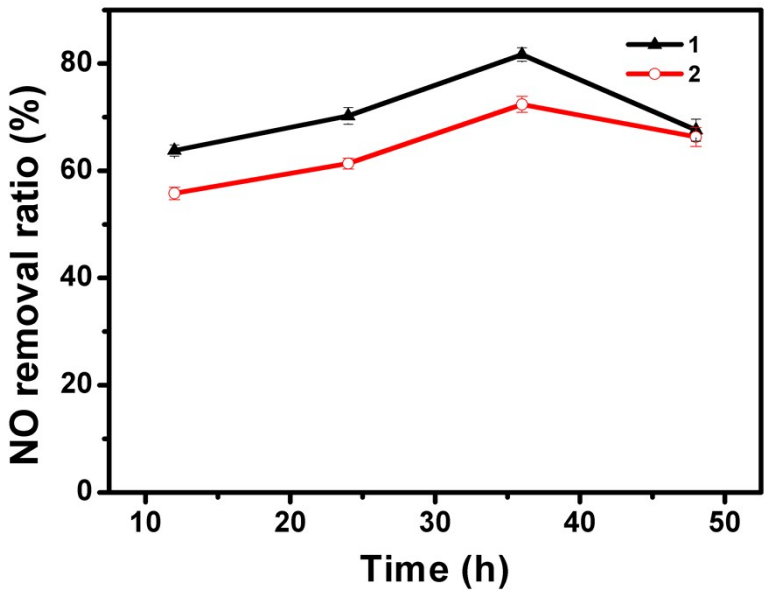

Figure S9 NO removal performances by Mn-***24***h-coated ceramic honeycombs using the actual motor as the pollution source. Reaction conditions: [NO] = 1~10 ppm, temperature = 24 °C, relative humidity = 70~72% and space velocity = 28000 $mL \cdot h^{-1} \cdot g^{-1}$ (1) and 32400 $mL \cdot h^{-1} \cdot g^{-1}$ (2). The loaded amount of Mn-***24***h was measured to be ~1wt% of the honeycomb.

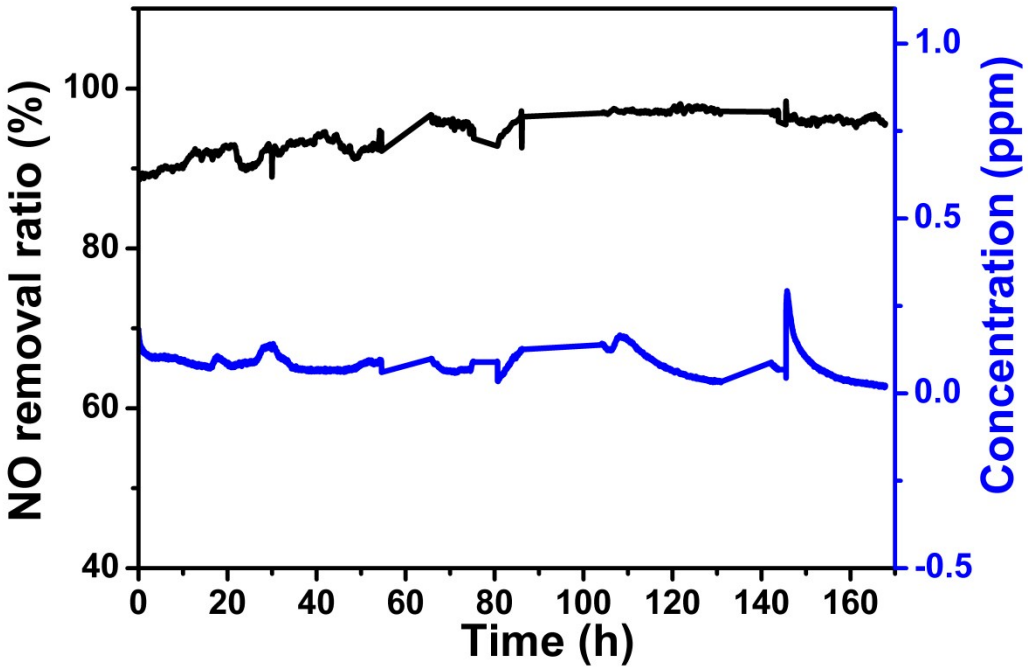

Figure S10 Time courses of NO removal on the used Mn-***24***h (black line) for 237 h with fresh air as the carrier gas and outlet NO_2 concentrations (blue line) during the test. Reaction conditions: [NO] = 10 ppm, balance = fresh air, temperature = 25 °C, relative humidity = 50~90% and space velocity = 120,000 $mL \cdot h^{-1} \cdot g^{-1}$.

Table S1 Pore structural parameters and the molar ratio of K/Mn of synthesized Mn-***t***h. [a] BET surface area; [b] BJH desorption average pore diameter; [c] BJH desorption cumulative pore volume.

Sample	**S_{BET}[a] (m^2/g)**	**D_{BJH}[b] (nm)**	**V_{BJH}[c] (cm^3/g)**	**K/Mn**
Mn-***8***h	114	3.7	0.11	0.323
Mn-***20***h	147	3.4	0.13	0.324
Mn-***24***h	166	4.2	0.18	0.307
Mn-***28***h	156	3.4	0.15	0.324
Mn-***48h***	141	4.6	0.20	0.329

Table S2 XPS result of the $O_\alpha/(O_\alpha+O_\beta)$ ratio in the synthesized Mn-***t***h, where O_α (531.2 eV) means the defect oxygen species and O_β (529.6 eV) represents lattice oxygen.

Catalysts	**$O_\alpha/(O_\alpha+O_\beta)$**
Mn-***8***h	35.4%
Mn-***24***h	52.0%
Mn-***48***h	24.4%
Mn-***24***h(200^{o}C)	29.8%

Table S3 XPS result of Mn 2p in the synthesized Mn-*t*h samples

Catalysts	**Mn 2p (eV)**			**Mn^{2+}: Mn^{3+}: Mn^{4+}**
	Mn^{2+}	**Mn^{3+}**	**Mn^{4+}**	
Mn-***8***h	641.2	642.2	644.5	4.1%:69.7%:26.2%
Mn-***24***h	641.2	642.2	644.5	1.4%:68.4%:30.2%
Mn-***48***h	641.2	642.2	644.5	2.5%:82.8%:14.7%
Mn-***24***h(200^{o}C)	641.2	642.2	644.5	3.1%:76.2%:20.7%
Mn-***24***h-used (dry)	641.2	642.2	644.5	4.4%:76.0%:19.6%
Mn-***24***h-used (humid)	641.2	642.2	644.5	2.6%:67.2%:30.2%